

# Dynamic mode decomposition for interconnected control systems

Byron Heersink, Michael A. Warren, and Heiko Hoffmann

**Abstract**—Dynamic mode decomposition (DMD) is a data-driven technique used for capturing the dynamics of complex systems. DMD has been connected to spectral analysis of the Koopman operator, and essentially extracts spatial-temporal modes of the dynamics from an estimate of the Koopman operator obtained from data. Recent work of Proctor, Brunton, and Kutz has extended DMD and Koopman theory to accommodate systems with control inputs: dynamic mode decomposition with control (DMDC) and Koopman with inputs and control (KIC). In this paper, we introduce a technique, called Network dynamic mode decomposition with control, or Network DMDC, which extends the DMDC to interconnected, or networked, control systems. Additionally, we provide an adaptation of Koopman theory for networks as a context in which to perform this algorithm. The Network DMDC method carefully analyzes the dynamical relationships only between components in systems which are connected in the network structure. By focusing on these direct dynamical connections and cutting out computation for relationships between unconnected components, this process allows for improvements in computational intensity and accuracy.

**Index Terms**—Koopman operator theory; System identification; Network analysis and control; Computational methods.

## I. INTRODUCTION

**D**YNAMIC mode decomposition (DMD) is a method developed by Schmid and Sesterhenn [1], [2] used in the model reduction and decomposition of complex dynamical systems. This data-driven method is performed on time series data of a given system and attempts to identify a linear model for the dynamics, which is ideally of reduced order. Then the prominent behavior of the system is extracted from the linear model’s eigenvectors, or “modes”, whose dynamics are governed simply by their corresponding eigenvalues.

It has been shown that DMD is strongly related to Koopman operator theory. Originally defined by Koopman in 1931 [3], the Koopman operator is a linear infinite-dimensional operator on the space of observables of any dynamical system, including nonlinear systems. The work of Mezić [4] was the first to apply the spectral analysis of the Koopman operator to the model reduction of systems. Later, Rowley et al. [5] fundamentally linked DMD to Koopman theory by showing that

This work was funded under DARPA contract N66001-16-C-4053. The views expressed are those of the authors and do not reflect the official policy or position of the Department of Defense or the U.S. Government. Distribution Statement ‘A’: Approved for Public Release, Distribution Unlimited.

B. Heersink was with HRL Laboratories, LLC, Malibu, CA 90265. He is now with the Department of Mathematics, The Ohio State University, 231 W. 18th Ave., Columbus, OH 43210 (e-mail: heersink.5@osu.edu).

M. A. Warren and H. Hoffmann are with HRL Laboratories, LLC, 3011 Malibu Canyon Rd., Malibu, CA 90265 (email: mawarren@hrl.com; hhoffmann@hrl.com).

DMD is essentially a method of approximating the Koopman operator and its spectral decomposition.

In recent years, DMD and Koopman theory has been applied to a variety of different fields. Its first and most notable application area is fluid dynamics. See, e.g., [5], [2], [6], [7], as well as [8] for a review. Other applications include power systems [9], [10], [11], [12], video processing [13], [14], [15], epidemiology [16], robotics [17], neuroscience [18], and finance [19]. Additionally, there has been a lot of effort to refine and advance DMD and Koopman theory themselves. In particular, DMD has been improved by Tu et al. [7] to what is recognized as its preeminent form. Examples of innovations building upon DMD and Koopman theory include extended and kernel DMD [20], [21], which seek to more accurately approximate the Koopman operator by incorporating measurements of appropriate nonlinear observables explicitly or implicitly through use of a kernel; multi-resolution DMD [22]; and the incorporation of sparsity [23], compression [24], and de-biasing [25].

Another recent extension of DMD that can be applied to dynamical systems with control inputs is the dynamic mode decomposition with control (DMDC) [26]. Similar to DMD, DMDC seeks to find a linear model which approximates the dynamics of a given control system using only data measurements of the state and inputs of the system. DMDC has been applied to modeling a rapidly pitching airfoil [27], and has been leveraged to produce a generalization of Koopman theory to incorporate control inputs [28]. Other efforts to extend Koopman theory to control systems are [29], [30], [31].

In this paper, we introduce a further extension of DMDC to interconnected, or networked, control systems. That is, we formulate a DMDC algorithm specialized for analyzing systems which are composed of smaller subsystems arranged in a network structure, where each subsystem corresponds to a node in the network, and the edges in the network represent the dynamical interactions between subsystems. We call this algorithm Network Dynamic Mode Decomposition with Control, or Network DMDC. We also adapt Koopman theory to networked control systems to provide a framework within which to apply the Network DMDC algorithm.

Examples of systems with a network structure include chemical reaction networks, epidemiological networks capturing the transmission of diseases through different spatial locations or groups, power system networks, and gene regulatory networks. The main idea behind the Network DMDC algorithm is to exploit, when possible, existing network structure in complex systems to yield improvements in computation intensity and precision over standard DMDC.

In Section II, we review background on standard Koopman theory, the dynamic mode decomposition, and their analogues incorporating inputs and control. Then in Section III, we extend dynamic mode decomposition and Koopman theory to networked systems. We then present some examples demonstrating the network DMDc algorithm and some of its benefits in Section IV. Finally, we provide concluding remarks in Section V.

## II. KOOPMAN THEORY AND DYNAMIC MODE DECOMPOSITION WITH CONTROL

### A. Koopman theory

In this section, we outline the basics of Koopman theory. The reader is referred to [5], [32] for more details. Let  $\mathcal{M}$  be a state space of a discrete dynamical system  $T : \mathcal{M} \rightarrow \mathcal{M}$ , whose evolving trajectories are sequences  $x_1, x_2, x_3, \dots$  in  $\mathcal{M}$  such that

$$x_{k+1} = T(x_k). \quad (1)$$

We define the Koopman operator as the operator  $\mathcal{K}$  that acts on scalar-valued observable functions  $g : \mathcal{M} \rightarrow \mathbb{R}$  according to

$$(\mathcal{K}g)(x) = g(T(x)).$$

We think of  $\mathcal{K}$  as a linear operator on a vector space of observables on  $\mathcal{M}$  that we denote by  $\mathcal{O}(\mathcal{M})$ , and which is commonly chosen to be a Hilbert space (e.g., the functions on  $\mathcal{M}$  which are square-integrable with respect to some measure). The main idea of the Koopman method is to analyze the dynamical system (1) through the behavior of the observables on the state space. In particular, the goal is to use data recording the value of various observables to find the eigenvalues and eigenfunctions of  $\mathcal{K}$ , which would then help us better understand the dynamics of the system. Assume  $\varphi_j : \mathcal{M} \rightarrow \mathbb{R}$ ,  $j = 1, 2, \dots$ , are the eigenfunctions of  $\mathcal{K}$  with corresponding eigenvalues  $\lambda_j \in \mathbb{C}$ ,  $j = 1, 2, \dots$ , so that

$$(\mathcal{K}\varphi_j)(x) = \lambda_j\varphi_j(x).$$

Then for a given (vertical) vector valued observable  $\mathbf{g} : \mathcal{M} \rightarrow \mathbb{R}^n$ , each of whose components lie in the span of the eigenfunctions, we can write

$$\mathbf{g}(x) = \sum_{j=1}^{\infty} \varphi_j(x) \mathbf{v}_j.$$

The operator  $\mathcal{K}$  then acts on  $\mathbf{g}$  according to

$$(\mathcal{K}\mathbf{g})(x) = \sum_{j=1}^{\infty} \lambda_j \varphi_j(x) \mathbf{v}_j.$$

The vectors  $\mathbf{v}_j$ , which are called the Koopman modes associated to  $\mathbf{g}$ , are the components of  $\mathbf{g}$  whose dynamics can be simply discerned from the corresponding eigenvalues  $\lambda_j$ , which contain growth or decay rates and the oscillation frequency of the modes.

Koopman theory is also defined for continuous-time dynamical systems. In this context,  $\mathcal{M}$  is a subset of Euclidean space

and the trajectories  $x = x(t)$  of the system are governed by a differential equation

$$\frac{dx}{dt} = F(x);$$

or more generally,  $\mathcal{M}$  can be a smooth manifold and the dynamics governed by a vector field on  $\mathcal{M}$ . (In both cases, we assume the trajectories  $x(t)$  are defined for all  $t \geq 0$ .) We then have the flow function  $\Phi : \mathcal{M} \times [0, \infty) \rightarrow \mathcal{M}$  mapping a pair  $(x, t) \in \mathcal{M} \times [0, \infty)$  to the point in  $\mathcal{M}$  obtained by following the dynamics of the system for time  $t$  starting at the point  $x$ . Then a semigroup of operators  $\{U^t : t \geq 0\}$  can be defined on observables  $f : \mathcal{M} \rightarrow \mathbb{R}$  by

$$(U^t f)(x) = f(\Phi(x, t)).$$

Since DMD-based methods are performed on data at a discrete set of times, it is useful to view the system as a discrete-time system by fixing a time increment  $\Delta t > 0$  and defining the map  $T : \mathcal{M} \rightarrow \mathcal{M}$  by

$$T(x) = \Phi(x, \Delta t);$$

the corresponding Koopman operator  $\mathcal{K}$  is then equal to  $U^{\Delta t}$ .

### B. Dynamic mode decomposition

We now describe how the spectral analysis of the Koopman operator can be done via dynamic mode decomposition. See [7] for more details.

We consider two sets of (vertical) data vectors  $\{z_1, \dots, z_m\}, \{y_1, \dots, y_m\} \subseteq \mathbb{R}^n$ . We think of these vectors as measurements on a dynamical system such that for every  $k$ ,  $\mathbf{y}_k$  is the measurement of the system that follows the measurement  $z_k$  after a fixed time increment independent of  $k$ . Our goal is to try to find a linear model for the dynamics so that

$$\mathbf{y}_k \approx \mathbf{A}z_k$$

for some matrix  $\mathbf{A}$ . In other words, defining the matrices

$$\mathbf{Z} = [z_1 \ z_2 \ \dots \ z_m] \text{ and } \mathbf{Y} = [y_1 \ y_2 \ \dots \ y_m],$$

we wish to have

$$\mathbf{Y} \approx \mathbf{A}\mathbf{Z}.$$

We define  $\mathbf{A}$  to be

$$\mathbf{A} = \mathbf{Y}\mathbf{Z}^\dagger,$$

where  $\mathbf{Z}^\dagger$  denotes the Moore-Penrose pseudoinverse of  $\mathbf{Z}$ . The matrix  $\mathbf{Y}\mathbf{Z}^\dagger$  is an ideal candidate for  $\mathbf{A}$  since it is the matrix minimizing  $\|\mathbf{A}\mathbf{Z} - \mathbf{Y}\|_F$ , where  $\|\cdot\|_F$  denotes the Frobenius norm. If  $\mathbf{Y} = \mathbf{A}\mathbf{Z}$ , then  $\mathbf{X} = \mathbf{A}$  is the solution of  $\mathbf{Y} = \mathbf{X}\mathbf{Z}$  minimizing  $\|\mathbf{X}\|_F$ . The dynamic mode decomposition of the pair  $(\mathbf{Z}, \mathbf{Y})$  is the eigendecomposition of the matrix  $\mathbf{A}$ . However, the necessary computations could be intensive if the system is sufficiently large, in which case one can consider a reduced-order model for  $\mathbf{A}$ . This is done by the following:

*Algorithm 1 (DMD [7]):*

- 1) Compute the reduced and appropriately truncated SVD of  $\mathbf{Z}$ :

$$\mathbf{Z} \approx \mathbf{U}\mathbf{\Sigma}\mathbf{V}^*.$$

2) Define the reduced-model  $\tilde{\mathbf{A}}$  for  $\mathbf{A}$  by

$$\tilde{\mathbf{A}} = \mathbf{U}^* \mathbf{A} \mathbf{U} = \mathbf{U}^* \mathbf{Y} \mathbf{V} \mathbf{\Sigma}^{-1}.$$

3) Compute the eigendecomposition of  $\tilde{\mathbf{A}}$ :

$$\tilde{\mathbf{A}} \mathbf{W} = \mathbf{W} \mathbf{\Lambda}, \quad \mathbf{\Lambda} = \text{diag}(\lambda_1, \dots, \lambda_r).$$

4) For each column  $\mathbf{w}$  of  $\mathbf{W}$  with corresponding eigenvalue  $\lambda \neq 0$ , compute the associated eigenvector  $\phi$  of  $\mathbf{A}$  according to

$$\phi = \lambda^{-1} \mathbf{Y} \mathbf{V} \mathbf{\Sigma}^{-1} \mathbf{w}$$

These  $\phi$  make up part of the eigendecomposition of  $\mathbf{A}$ , forming the columns of a matrix  $\Phi$  such that

$$\mathbf{A} \Phi \approx \Phi \mathbf{\Lambda}.$$

In the context of Koopman theory as outlined in the previous section, the DMD algorithm is applied to the data

$$\mathbf{z}_k = \mathbf{g}(x_k), \quad \mathbf{y}_k = \mathbf{g}(w_k), \quad k = 1, \dots, m$$

where  $x_1, \dots, x_m, w_1, \dots, w_m \in \mathcal{M}$  is such that  $w_k = T(x_k)$ , and  $\mathbf{g}$  is a vector of observables as defined above. The eigendecomposition  $(\mathbf{\Lambda}, \Phi)$  resulting from the DMD then gives an approximation of the eigenvalues and Koopman modes of the Koopman operator  $\mathcal{K}$  with respect to the observable  $\mathbf{g}$ .

### C. Koopman theory and dynamic mode decomposition with control

Next, we outline the work of Proctor et al. [26], [28] in generalizing Koopman theory and the DMD to incorporate control inputs. Because of the generality and concrete framework of Koopman theory, we present the dynamic mode decomposition with control [26] as encompassed within Koopman theory with inputs and control (KIC) [28].

We consider a discrete control system  $T : \mathcal{M} \times \mathcal{U} \rightarrow \mathcal{M}$ , where  $\mathcal{M}$  is the state space of the system as above, and  $\mathcal{U}$  is the space of controls. The trajectories of this system are sequences  $x_1, x_2, \dots$  in  $\mathcal{M}$ , with corresponding input sequences  $u_1, u_2, \dots$  in  $\mathcal{U}$  such that

$$x_{k+1} = T(x_k, u_k).$$

In [28], the Koopman operator  $\mathcal{K}$  in this context acts on observables  $g : \mathcal{M} \times \mathcal{U} \rightarrow \mathbb{R}$  according to

$$(\mathcal{K}g)(x, u) = g(T(x, u), *),$$

where  $*$  can be chosen in different ways depending on how one wishes to treat the inputs. One can then attempt to analyze  $\mathcal{K}$  as an operator on  $\mathcal{M} \times \mathcal{U}$  via DMD. Here, however, we restrict the domain of  $\mathcal{K}$  to observables on  $\mathcal{M}$  so that for a given observable  $g : \mathcal{M} \rightarrow \mathbb{R}$ , we have

$$(\mathcal{K}g)(x, u) = g(T(x, u));$$

and we avoid the ambiguity of having to choose  $*$  above. We think of  $\mathcal{K}$  as a linear operator mapping a vector space of observables  $\mathcal{O}(\mathcal{M})$  on  $\mathcal{M}$  to another vector space of observables  $\mathcal{O}(\mathcal{M} \times \mathcal{U})$  on  $\mathcal{M} \times \mathcal{U}$ .

As in the autonomous case, one can adapt Koopman theory to continuous-time control systems. In this context,  $\mathcal{M}$  and  $\mathcal{U}$  are Euclidean spaces and the dynamics of the state  $x = x(t)$  is governed by a differential equation

$$\frac{dx}{dt} = F(x, u),$$

where  $u = u(t)$  is an input signal. (One can more generally consider when  $\mathcal{M}$  and  $\mathcal{U}$  are smooth manifolds.) Then for each fixed input  $u \in \mathcal{U}$ , one has a function  $\Phi_u : \mathcal{M} \times [0, \infty) \rightarrow \mathcal{M}$  yielding the flow of points in  $\mathcal{M}$  assuming the input signal is fixed at  $u$ . These functions in turn induce operators  $\{U_u^t : t \geq 0, u \in \mathcal{U}\}$  defined by

$$(U_u^t g)(x) = g(\Phi_u(x, t)).$$

One can then define the Koopman operator  $\mathcal{K}$  by

$$(\mathcal{K}g)(x, u) = (U_u^{\Delta t} g)(x)$$

for some fixed  $\Delta t > 0$ . Note that in doing this, we must restrict the control signals we consider to those which are constant on time intervals of length  $\Delta t$ .

Now let  $\mathbf{g} : \mathcal{M} \rightarrow \mathbb{R}^n$  be a vector of observables on  $\mathcal{M}$  and  $\mathbf{h} : \mathcal{U} \rightarrow \mathbb{R}^l$  a vector of observables on  $\mathcal{U}$ . Also let  $(x_1, u_1, w_1), (x_2, u_2, w_2), \dots, (x_m, u_m, w_m)$  be triples such that  $w_k = T(x_k, u_k)$  and define the matrices

$$\begin{aligned} \mathbf{Z} &= [\mathbf{z}_1 \ \mathbf{z}_2 \ \cdots \ \mathbf{z}_m] = [\mathbf{g}(x_1) \ \mathbf{g}(x_2) \ \cdots \ \mathbf{g}(x_m)] \\ \mathbf{Y} &= [\mathbf{y}_1 \ \mathbf{y}_2 \ \cdots \ \mathbf{y}_m] = [\mathbf{g}(w_1) \ \mathbf{g}(w_2) \ \cdots \ \mathbf{g}(w_m)] \\ \mathbf{\Gamma} &= [\boldsymbol{\gamma}_1 \ \boldsymbol{\gamma}_2 \ \cdots \ \boldsymbol{\gamma}_m] = [\mathbf{h}(u_1) \ \mathbf{h}(u_2) \ \cdots \ \mathbf{h}(u_m)] \end{aligned}$$

The DMDc algorithm can then be applied in an effort to find a matrices  $\mathbf{A}$  and  $\mathbf{B}$  such that

$$\mathbf{g}(w_k) \approx \mathbf{A} \mathbf{g}(x_k) + \mathbf{B} \mathbf{h}(u_k).$$

In other words, if we let  $\mathbf{\Omega} = \begin{bmatrix} \mathbf{Z} \\ \mathbf{\Gamma} \end{bmatrix}$ , we wish for  $\mathbf{G} = [\mathbf{A} \ \mathbf{B}]$  to satisfy

$$\mathbf{Y} \approx \mathbf{G} \mathbf{\Omega}.$$

We define  $\mathbf{G}$  to be

$$\mathbf{G} = [\mathbf{A} \ \mathbf{B}] = \mathbf{Y} \mathbf{\Omega}^\dagger.$$

The DMDc of the triple  $(\mathbf{Z}, \mathbf{Y}, \mathbf{\Gamma})$  is the eigendecomposition of the matrix  $\mathbf{A}$ . For ease of computation for large systems, the DMDc algorithm can also compute a reduced-order model for  $\mathbf{G}$ , and then the eigendecomposition for the corresponding reduced-order model of  $\mathbf{A}$ , which gives approximate dynamic modes for the system. This algorithm is described as follows: *Algorithm 2 (DMDc [26]):*

1) Compute the reduced and appropriately truncated SVD of  $\mathbf{\Omega}$ :

$$\mathbf{\Omega} \approx \mathbf{U} \mathbf{\Sigma} \mathbf{V}^*.$$

and let  $p$  be the truncation value so that  $\mathbf{U} \in \mathbb{R}^{(n+l) \times p}$ ,  $\mathbf{\Sigma} \in \mathbb{R}^{p \times p}$ , and  $\mathbf{V}^* \in \mathbb{R}^{p \times m}$ . Note that

$$\mathbf{G} \approx \mathbf{Y} \mathbf{V} \mathbf{\Sigma}^{-1} \mathbf{U}^*, \text{ i.e.,}$$

$$[\mathbf{A} \ \mathbf{B}] \approx [\mathbf{Y} \mathbf{V} \mathbf{\Sigma}^{-1} \mathbf{U}_1^* \ \mathbf{Y} \mathbf{V} \mathbf{\Sigma}^{-1} \mathbf{U}_2^*],$$

where  $\mathbf{U}_1^* \in \mathbb{R}^{p \times n}$  and  $\mathbf{U}_2^* \in \mathbb{R}^{p \times l}$  such that  $\mathbf{U}^* = [\mathbf{U}_1^* \ \mathbf{U}_2^*]$ .

- 2) Compute the reduced and appropriately truncated SVD of  $Y$ :

$$Y \approx \hat{U} \hat{\Sigma} \hat{V}^*.$$

and let  $r$  be the truncation value so that  $\hat{U} \in \mathbb{R}^{n \times r}$ ,  $\hat{\Sigma} \in \mathbb{R}^{r \times r}$ , and  $\hat{V}^* \in \mathbb{R}^{r \times m}$ .

- 3) Compute the reduced-order model  $[\tilde{A} \ \tilde{B}]$  of  $[A \ B]$  as

$$[\tilde{A} \ \tilde{B}] = [\hat{U}^* Y V \Sigma^{-1} U_1^* \hat{U} \quad \hat{U}^* Y V \Sigma^{-1} U_2^*].$$

(Intuitively, we have  $\tilde{A} \approx \hat{U}^* A \hat{U}$  and  $\tilde{B} \approx \hat{U}^* B$ .)

- 4) Compute the eigendecomposition for  $\tilde{A}$ :

$$\tilde{A} W = W \Lambda$$

- 5) Compute the approximate eigenvectors of  $A$  associated to the columns of  $W$ , forming the columns of a matrix  $\Phi$ :

$$\Phi = Y V \Sigma^{-1} U_1^* \hat{U} W.$$

The reduced-order model for the state space measurements is then  $\mathbb{R}^r$ , and we think of the reduced-order measurement corresponding to  $z \in \mathbb{R}^n$  as  $\tilde{z} = \hat{U}^* z \in \mathbb{R}^r$ . On the other hand, the reduced-order measurement  $\tilde{z}$  relates to the original measurement as  $z = \hat{U} \tilde{z}$ . (Note  $\hat{U}^*$  is a left inverse for  $\hat{U}$ .)

### III. EXTENSION TO NETWORKED SYSTEMS

Now that we have outlined the DMDc algorithm and Koopman theory with control inputs, we can explain their extension to networked systems. As before, we present Network DMDc in the context of Koopman theory due to its generality.

#### A. Networked control systems

We begin by defining precisely what we mean by a networked control system. Let  $G$  be a directed graph with vertices partitioned into two disjoint sets  $N = \{v_1, v_2, \dots, v_\nu\}$  and  $I = \{e_1, \dots, e_\mu\}$  such that the only edges connected to the vertices in  $I$  are directed outward from those vertices. We associate each vertex  $w$  in  $N \cup I$  with a set  $P_w$  that represents a component of the system. If  $w \in N$ , then  $P_w$  is a component of the state space of the system, while if  $w \in I$ , then  $P_w$  is a component of the input space. The entire state space is therefore  $\mathcal{M} := \prod_{v \in N} P_v$ , and the entire input space is  $\mathcal{U} := \prod_{e \in I} P_e$ . (The set  $I$  is allowed to be empty, in which case the system is autonomous.)

For  $v \in N$ , let  $I_v \subseteq N \cup I$  be the set of vertices having an outgoing edge pointing into  $v$ . We then have the transition function  $T_v : P_v \times \prod_{w \in I_v} P_w \rightarrow P_v$  which governs the behavior of component  $P_v$ : if  $(x_w)_{w \in N \cup I}$  are the state and input components of the system at a particular time, the  $P_v$  component of the state at the following time is  $T_v(x_v, (x_w)_{w \in I_v})$ . Thus the edges of  $G$  represent the pattern of influence the different components of the system have on one another. The individual transition functions can then be composed to produce the transition function  $T : \mathcal{M} \times \mathcal{U} \rightarrow \mathcal{M}$  of the entire system. Thus the graph  $G$ , the state and input spaces  $P_w$ , and the transition functions  $T_v$  define a networked control system.

For example, consider the simple network depicted in Figure 1. It has state vertices  $N = \{v_1, v_2\}$  and input vertices

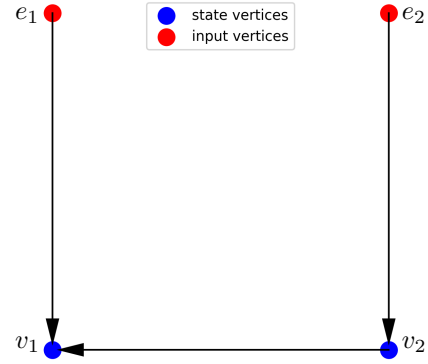


Fig. 1. A simple network with 2 state vertices and 2 input vertices

$I = \{e_1, e_2\}$ . Since there are edges from  $v_2$  and  $e_1$  to  $v_1$ , the transition function governing the dynamics of the  $v_1$ -component is of the form  $T_{v_1} : P_{v_1} \times P_{v_2} \times P_{e_1} \rightarrow P_{v_1}$ . Similarly, the edge from  $e_2$  to  $v_2$  implies that the transition function for  $v_2$  is of the form  $T_{v_2} : P_{v_2} \times P_{e_2} \rightarrow P_{v_2}$ . Thus the complete transition function of the system  $T : \prod_{j=1,2} P_{v_j} \times \prod_{j=1,2} P_{e_j} \rightarrow \prod_{j=1,2} P_{v_j}$  is given by

$$T(x_{v_1}, x_{v_2}, x_{e_1}, x_{e_2}) = (T_{v_1}(x_{v_1}, x_{v_2}, x_{e_1}), T_{v_2}(x_{v_2}, x_{e_2})).$$

One can consider analogous continuous-time networked systems as well. Then all  $P_w$  are Euclidean spaces or smooth manifolds, and each transition function  $T_v$  is replaced by a differential equation of the form

$$\frac{dx_v}{dt} = F_v(x_v, (x_w)_{w \in I_v}),$$

or an appropriate map from  $P_v \times \prod_{w \in I_v} P_w$  to the tangent bundle of  $P_v$ . Such a system can then be approximated by a discrete-time networked system by a process similar to that given in Section II-C. Only an approximation can be made in general due to possible dependence of state components on other state components that change continuously, which should be constant in time intervals over which the system is discretized.

#### B. Koopman theory for networks

In this section, we provide a Koopman theory framework for the network systems we defined in the previous section. First, for each  $v \in N$ , we consider the transition function  $T_v : P_v \times \prod_{w \in I_v} P_w \rightarrow P_v$  as a discrete control system with state space  $P_v$  and input space  $\prod_{w \in I_v} P_w$ . We can then define the corresponding Koopman operator  $\mathcal{K}_v$  as in Section II-C so that for  $g : P_v \rightarrow \mathbb{R}$ , we have

$$(\mathcal{K}_v g)(x_v, (x_w)_{w \in I_v}) = g(T_v(x_v, (x_w)_{w \in I_v})).$$

So we think of  $\mathcal{K}_v$  as an operator between vector spaces of observables  $\mathcal{O}(P_v) \rightarrow \mathcal{O}(P_v \times \prod_{w \in I_v} P_w)$ .

Analogous to how the transition functions  $T_v$  compose to form  $T$ , we wish to see how we can compose the operators  $\mathcal{K}_v$  to obtain the Koopman operator corresponding to  $T$ . First, by composing it with the natural inclusion

$$\mathcal{O} \left( P_v \times \prod_{w \in I_v} P_w \right) \rightarrow \mathcal{O}(\mathcal{M} \times \mathcal{U}), \quad (2)$$

(assuming the former is a subspace of the latter) we may view  $\mathcal{K}_v$  as an operator from  $\mathcal{O}(P_v)$  to  $\mathcal{O}(\mathcal{M} \times \mathcal{U})$ . Then taking the tensor product of  $\mathcal{K}_v$  over  $v \in N$  yields an operator

$$\bigotimes_{v \in N} \mathcal{K}_v : \bigotimes_{v \in N} \mathcal{O}(P_v) \rightarrow \mathcal{O}(\mathcal{M} \times \mathcal{U}).$$

We wish to identify the tensor product  $\bigotimes_{v \in N} \mathcal{O}(P_v)$  with an appropriate space of observables on  $\prod_{v \in N} P_v$ , ideally  $\mathcal{O}(\mathcal{M})$ , via the identification of  $\bigotimes_{v \in N} f_v \in \bigotimes_{v \in N} \mathcal{O}(P_v)$  with  $\prod_{v \in N} f_v$  as a function on  $\mathcal{M}$ . If this identification can be made, we can then identify  $\bigotimes_{v \in N} \mathcal{K}_v$  with the Koopman operator  $\mathcal{K}$  of the entire system.

Some assumptions under which this process works is when for each  $w \in N \cup I$ ,  $\mathcal{O}(P_w) = L^2(P_w, \mu_w)$ , where  $\mu_w$  is a finite measure on  $P_w$ , and  $\mathcal{K}_v$  is bounded. In this case, the inclusions (2) are valid, and the appropriate completion of  $\bigotimes_{v \in N} L^2(P_v)$  is identified with  $L^2(\mathcal{M}, \bigotimes_{v \in N} \mu_v)$ . (See for instance [33, Example 2.6.11].)

### C. Network DMDC

The previous section provides a way of decomposing the Koopman operator of a networked system into smaller operators. This gives us a framework in which to formulate our Network DMDC algorithm. The basic idea is to apply the original DMDC algorithm to each operator  $\mathcal{K}_v$  to get a ‘‘local’’ analysis of the behavior of the system at each state space component  $P_v$  in response to the components it is immediately influenced by. The resulting linear control systems are then composed to obtain a linear system approximating the whole network.

First of all, let  $(x_1, u_1, w_1), \dots, (x_m, u_m, w_m)$  be triples in  $\mathcal{M} \times \mathcal{U} \times \mathcal{M}$  such that  $w_k = T(x_k, u_k)$ , and denote the  $P_{v_j}$  component of  $x_k$  and  $y_k$  as  $x_{k,j}$  and  $y_{k,j}$ , respectively, and the  $P_{e_j}$  component of  $u_k$  as  $u_{k,j}$ . Then let  $\mathbf{g} : \prod_{j=1}^{\nu} P_{v_j} \rightarrow \mathbb{R}^n$  and  $\mathbf{h} : \prod_{j=1}^{\mu} P_{e_j} \rightarrow \mathbb{R}^l$  be observables of the form

$$\mathbf{g} = \begin{bmatrix} \mathbf{g}_1 \\ \vdots \\ \mathbf{g}_\nu \end{bmatrix} \quad \text{and} \quad \mathbf{h} = \begin{bmatrix} \mathbf{h}_1 \\ \vdots \\ \mathbf{h}_\mu \end{bmatrix}, \quad \text{where}$$

$$\mathbf{g}_j : P_{v_j} \rightarrow \mathbb{R}^{n_j}, \quad j = 1, \dots, \nu$$

$$\mathbf{h}_j : P_{e_j} \rightarrow \mathbb{R}^{l_j}, \quad j = 1, \dots, \mu.$$

The first step of the Network DMDC process is to form subsystems centered at each state vertex. Specifically, for each  $v_j \in N$ , we consider the ‘‘local subsystem’’ consisting of  $v_j$ , which we think of as the state vertex of the subsystem, and

$$I_j = \{v_{k_j(1)}, v_{k_j(2)}, \dots, v_{k_j(\alpha_j)}, e_{\ell_j(1)}, e_{\ell_j(2)}, \dots, e_{\ell_j(\beta_j)}\},$$

which we think of as the set of input vertices of the subsystem. Next, define the observable  $\mathbf{h}^{(j)}$  on  $\prod_{w \in I_j} P_w$  by

$$\mathbf{h}^{(j)} = \begin{bmatrix} \mathbf{g}_{k_j(1)} \\ \vdots \\ \mathbf{g}_{k_j(\alpha_j)} \\ \mathbf{h}_{\ell_j(1)} \\ \vdots \\ \mathbf{h}_{\ell_j(\beta_j)} \end{bmatrix}.$$

We then define the triple  $(\mathbf{Z}_j, \mathbf{\Gamma}_j, \mathbf{Y}_j)$  by

$$\begin{aligned} \mathbf{Z}_j &= [\mathbf{g}_j(x_{1,j}) \quad \mathbf{g}_j(x_{2,j}) \quad \cdots \quad \mathbf{g}_j(x_{m,j})] \\ \mathbf{Y}_j &= [\mathbf{g}_j(w_{1,j}) \quad \mathbf{g}_j(w_{2,j}) \quad \cdots \quad \mathbf{g}_j(w_{m,j})] \\ \mathbf{\Gamma}_j &= [\mathbf{h}^{(j)}(\mathbf{u}_1^{(j)}) \quad \mathbf{h}^{(j)}(\mathbf{u}_2^{(j)}) \quad \cdots \quad \mathbf{h}^{(j)}(\mathbf{u}_m^{(j)})], \end{aligned}$$

where  $\mathbf{u}_k^{(j)} = (x_{k,k_j(1)}, \dots, x_{k,k_j(\alpha_j)}, u_{k,\ell_j(1)}, \dots, u_{k,\ell_j(\beta_j)})$ .

We analyze the subsystem centered at  $v_j$  by applying the DMDC to  $(\mathbf{Z}_j, \mathbf{\Gamma}_j, \mathbf{Y}_j)$ . In the case where a reduced-order model is not sought, the DMDC yields matrices  $\mathbf{A}_{j,j}$ ,  $\mathbf{B}_j$  that model the behavior of  $\mathbf{g}_j$  by linear control:

$$\mathbf{g}_j(x_{k+1,j}) \approx \mathbf{A}_{j,j} \mathbf{g}_j(x_{k,j}) + \mathbf{B}_j \mathbf{h}^{(j)}(\mathbf{u}_k^{(j)}),$$

which we can rewrite as

$$\begin{aligned} \mathbf{g}_j(x_{k+1,j}) &\approx \mathbf{A}_{j,j} \mathbf{g}_j(x_{k,j}) + \sum_{i=1}^{\alpha_j} \mathbf{A}_{j,k_j(i)} \mathbf{g}_{k_j(i)}(x_{k,k_j(i)}) \\ &\quad + \sum_{i=1}^{\beta_j} \mathbf{B}_{j,\ell_j(i)} \mathbf{h}_{\ell_j(i)}(u_{k,\ell_j(i)}). \end{aligned}$$

Repeating this process for every  $j = 1, \dots, \nu$  gives us a linear control approximation for each local subsystem, which we can combine to obtain an approximation for the whole system. Indeed, we can define  $\mathbf{A}_{j,i}$  to be the zero matrix in  $\mathbb{R}^{n_j \times n_i}$  if there is not an edge in  $G$  from  $v_i$  to  $v_j$ , and similarly let  $\mathbf{B}_{j,i}$  be zero in  $\mathbb{R}^{n_j \times l_i}$  if there is not an edge from  $e_i$  to  $v_j$ . We then have

$$\mathbf{g}(x_{k+1}) \approx \mathbf{A} \mathbf{g}(x_k) + \mathbf{B} \mathbf{h}(u_k),$$

where

$$\mathbf{A} = \begin{bmatrix} \mathbf{A}_{1,1} & \mathbf{A}_{1,2} & \cdots & \mathbf{A}_{1,\nu} \\ \mathbf{A}_{2,1} & \mathbf{A}_{2,2} & \cdots & \mathbf{A}_{2,\nu} \\ \vdots & \vdots & \ddots & \vdots \\ \mathbf{A}_{\nu,1} & \mathbf{A}_{\nu,2} & \cdots & \mathbf{A}_{\nu,\nu} \end{bmatrix},$$

$$\mathbf{B} = \begin{bmatrix} \mathbf{B}_{1,1} & \mathbf{B}_{1,2} & \cdots & \mathbf{B}_{1,\mu} \\ \mathbf{B}_{2,1} & \mathbf{B}_{2,2} & \cdots & \mathbf{B}_{2,\mu} \\ \vdots & \vdots & \ddots & \vdots \\ \mathbf{B}_{\nu,1} & \mathbf{B}_{\nu,2} & \cdots & \mathbf{B}_{\nu,\mu} \end{bmatrix}.$$

In the case where a reduced-order model is sought in the applications of the DMDC, then for each  $j = 1, \dots, \nu$ , the process yields matrices

$$\tilde{\mathbf{A}}_{j,j} = \hat{\mathbf{U}}_j^* \mathbf{A}_{j,j} \hat{\mathbf{U}}_j,$$

$$\tilde{\mathbf{A}}_{j,k_j(i)} = \hat{\mathbf{U}}_j^* \mathbf{A}_{j,k_j(i)},$$

$$\tilde{\mathbf{B}}_{j,\ell_j(i)} = \hat{\mathbf{U}}_j^* \mathbf{B}_{j,\ell_j(i)},$$

where  $\hat{\mathbf{U}}_j$  is the matrix of left singular vectors in the SVD of  $\begin{bmatrix} \mathbf{Z}_j \\ \mathbf{\Gamma}_j \end{bmatrix}$  that was chosen in the DMDC application. These matrices satisfy

$$\begin{aligned} \tilde{\mathbf{g}}_j(x_{k+1,j}) &\approx \tilde{\mathbf{A}}_{j,j} \tilde{\mathbf{g}}_j(x_{k,j}) + \sum_{i=1}^{\alpha_j} \tilde{\mathbf{A}}_{j,k_j(i)} \mathbf{g}_{k_j(i)}(x_{k,k_j(i)}) \\ &\quad + \sum_{j=1}^{\beta_j} \tilde{\mathbf{B}}_{j,\ell_j(i)} \mathbf{h}_{\ell_j(i)}(u_{k,\ell_j(i)}), \end{aligned}$$

where  $\tilde{g}_j := \hat{U}_j^* g_j$ . If we then let  $\tilde{A}_{j,k} := \bar{A}_{j,k} \hat{U}_k$ , we have

$$\begin{aligned} \tilde{g}_j(x_{k+1,j}) &\approx \tilde{A}_{j,j} \tilde{g}_j(x_{k,j}) + \sum_{i=1}^{\alpha_j} \tilde{A}_{j,k_j(i)} \tilde{g}_{k_j(i)}(x_{k,k_j(i)}) \\ &\quad + \sum_{j=1}^{\beta_j} \tilde{B}_{j,\ell_j(i)} h_{\ell_j(i)}(u_{k,\ell_j(i)}). \end{aligned}$$

Also letting  $\tilde{A}_{j,i}$  be the zero matrix of the appropriate size if there is not an edge in  $G$  from  $v_i$  to  $v_j$ , we obtain a reduced-order approximation of the entire system:

$$\tilde{g}(x_{k+1}) \approx \tilde{A} \tilde{g}(x_k) + \tilde{B} h(u_k),$$

where

$$\tilde{g} = \begin{bmatrix} \tilde{g}_1 \\ \tilde{g}_2 \\ \vdots \\ \tilde{g}_\nu \end{bmatrix}, \quad A = \begin{bmatrix} \tilde{A}_{1,1} & \tilde{A}_{1,2} & \cdots & \tilde{A}_{1,\nu} \\ \tilde{A}_{2,1} & \tilde{A}_{2,2} & \cdots & \tilde{A}_{2,\nu} \\ \vdots & \vdots & \ddots & \vdots \\ \tilde{A}_{\nu,1} & \tilde{A}_{\nu,2} & \cdots & \tilde{A}_{\nu,\nu} \end{bmatrix},$$

$$\text{and } B = \begin{bmatrix} \tilde{B}_{1,1} & \tilde{B}_{1,2} & \cdots & \tilde{B}_{1,\mu} \\ \tilde{B}_{2,1} & \tilde{B}_{2,2} & \cdots & \tilde{B}_{2,\mu} \\ \vdots & \vdots & \ddots & \vdots \\ \tilde{B}_{\nu,1} & \tilde{B}_{\nu,2} & \cdots & \tilde{B}_{\mu,\nu} \end{bmatrix}.$$

#### IV. EXAMPLES

We now illustrate the Network DMDC and its main advantages with a few examples.

*Example 1 (A simple linear example):* In this example, we illustrate in detail how the Network DMDC is applied to the simple network described in Section III-A and depicted in Figure 1. Assume all state and input spaces are the real line  $\mathbb{R}$ , and that the dynamics is linear so that

$$\begin{aligned} T_{v_1}(x_{v_1}, x_{v_2}, x_{e_1}) &= a_{1,1}x_{v_1} + a_{1,2}x_{v_2} + b_1x_{e_1}, \text{ and} \\ T_{v_2}(x_{v_2}, x_{e_2}) &= a_{2,2}x_{v_2} + b_2x_{e_2} \end{aligned}$$

for fixed  $a_{i,j}, b_i \in \mathbb{R}$ . Specifically, we set these constants as follows:

$$(a_{1,1}, a_{1,2}, a_{2,2}, b_1, b_2) = (1.2, -0.5, 0.8, 1, 1).$$

We shall see that the Network DMDC algorithm can recover the linear dynamics of the system.

To perform Network DMDC, we simulate the system for 3 time steps, yielding data for 4 total time instances. With the notation of Section III-C, we start with the initial state  $(x_{1,1}, x_{1,2}) = (2, 5)$  and use the randomly generated sequences of input values  $(u_{1,1}, u_{2,1}, u_{3,1}) = (0.2, 0.4, 0.8)$  (for  $e_1$ ) and  $(u_{1,2}, u_{2,2}, u_{3,2}) = (0.3, 0.1, 0.3)$  (for  $e_2$ ). Letting all observables  $g_j, h_j$  be the identity, and  $x_j = w_{j-1}$  for  $j = 2, 3, 4$ , we get the following data matrices:

$$\begin{aligned} Z_1 &= [2 \quad 0.1 \quad -1.63] & Z_2 &= [5 \quad 4.3 \quad 3.54] \\ Y_1 &= [0.1 \quad -1.63 \quad -2.926] & Y_2 &= [4.3 \quad 3.54 \quad 3.132] \\ \Gamma_1 &= \begin{bmatrix} 5 & 4.3 & 3.54 \\ 0.2 & 0.4 & 0.8 \end{bmatrix} & \Gamma_2 &= [0.3 \quad 0.1 \quad 0.3]. \end{aligned}$$

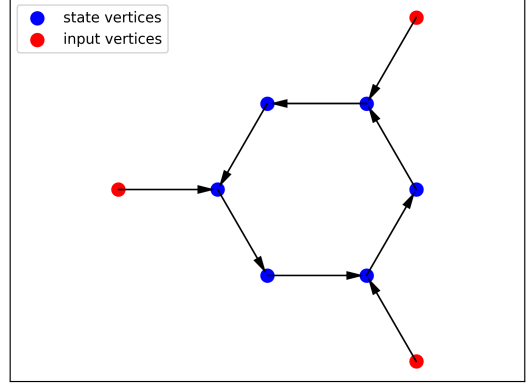


Fig. 2. Circular network with 6 state vertices and 3 input vertices

Performing DMDC on the triples  $(Z_j, Y_j, \Gamma_j)$  yields

$$\begin{aligned} [a_{1,1} \quad a_{1,2} \quad b_1] &= Y_1 \begin{bmatrix} Z_1 \\ \Gamma_1 \end{bmatrix}^\dagger = [1.2 \quad -0.5 \quad 1] \\ [a_{2,2} \quad b_2] &= Y_2 \begin{bmatrix} Z_2 \\ \Gamma_2 \end{bmatrix}^\dagger = [0.8 \quad 1], \end{aligned}$$

thus recovering the dynamics.

Note that applying the regular DMDC algorithm to the above data does not accurately recover the dynamics. However, regular DMDC can possibly recover them if it is performed on data from a simulation spanning 5 time instances. We explain why this happens after the next example, which is a more dramatic illustration of this phenomenon.

*Example 2 (Circular networks):* We now consider a circular network with state vertices  $v_1, \dots, v_n$  such that for  $j = 1, \dots, n-1$ , there is a directed edge from  $v_j$  to  $v_{j+1}$ , and there is another edge from  $v_n$  to  $v_1$ . Additionally, the network has input vertices  $e_1, \dots, e_m$ , ( $m \leq n$ ) each having a single edge pointing to one state vertex. On the other hand, there is at most one edge pointing to a given state vertex from an input vertex. Figure 2 illustrates an example of this type of network. As in the previous example,  $P_w = \mathbb{R}$  for all  $w \in N \cup I$ , and the dynamics is linear so that for a given  $v_j \in N$ , we have

$$T_{v_j}(x_{v_j}, x_{v_{j-1(\bmod n)}}, x_{e_k}) = a_j x_{v_j} + b_j x_{v_{j-1(\bmod n)}} + c_j x_{e_k}.$$

Here  $k$  is the index such that  $e_k$  is connected to  $v_j$ . If no input vertex is connected to  $v_j$ , then the term  $c_j x_{e_k}$  above is ignored.

For several networks of this type having various sizes and parameters, we tested the standard DMDC (or DMD in cases without inputs) and Network DMDC algorithms by seeing how effectively both can recover their linear dynamics. In particular, we performed simulations of the network of various time lengths, resulting in triples  $(x_1, u_1, w_1), \dots, (x_m, u_m, w_m) \in \mathcal{M} \times \mathcal{U} \times \mathcal{M}$  with  $x_j = w_{j-1}$  for  $j \geq 2$ , and where the input values  $u_k$  were randomly sampled from a uniform distribution on a finite interval. Then for each simulation, we obtained the matrices  $[A \ B]$  that result from applying both algorithms to the data  $(Z_j, Y_j, \Gamma_j)$  following from letting all observables  $g_j, h_j$  be the identity. We then measured how close the matrices were to the matrix giving the actual dynamics of the

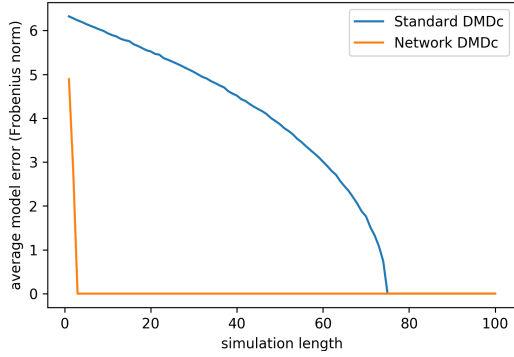


Fig. 3. The average error in the results of the standard and network DMDc applied to 20 circular networks of 50 state vertices 25 input vertices

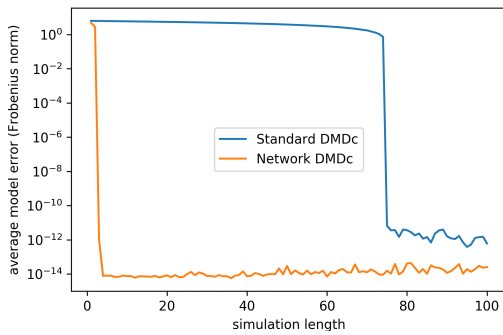


Fig. 4. Log scale of Figure 3

network. The measure of closeness used was the Frobenius norm of the difference of the two matrices.

The Network DMDc was consistently more accurate than the standard DMDc throughout these tests, and in particular required simulations of significantly shorter length to recover the actual dynamics to within a negligible error. For instance, Figures 3 and 4 depict the average error in the models generated by the network and standard DMDc algorithms for 20 circular networks having 50 state vertices, every other of which is connected to an input vertex, analogous to the smaller network in Figure 2. For each network, the parameters  $a_j, b_j, c_j$  were chosen randomly from a uniform distribution on the interval  $[-1, 1]$ , and the values for the input vertices were chosen from a uniform distribution on  $[-10, 10]$ . (Note that for each simulation, the input data for the standard DMDc was the same as that for the network DMDc, so that the accuracy comparison was fair.)

For the simulations depicted by Figures 3 and 4, the standard DMDc algorithm required a simulation length of  $m = 75$  (that is, concluding with the calculation of  $w_m = T(x_m, u_m)$ ) to recapture the actual dynamics to within negligible error, whereas the Network DMDc algorithm required only a simulation length of  $m = 3$ . Note that 75 is the dimension of each system defined by one entire network, and 3 is the maximum dimension of each “local subsystem” consisting of one state vertex  $v$  and all the state and input vertices having edges pointing to  $v$ . (Recall that the Network DMDc is based on applying the regular DMDc to each such local subsystem.)

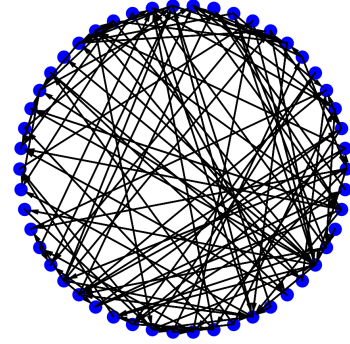


Fig. 5. Erdős-Renyi random directed network with  $n = 50$  and  $p = 0.05$

This makes sense because, in the first case, a simulation length of 75 would make each matrix  $\Omega = \begin{bmatrix} Z \\ \Gamma \end{bmatrix}$  a square matrix, and in the second case, a simulation length of 3 would make the matrices  $\begin{bmatrix} Z_j \\ \Gamma_j \end{bmatrix}$  square or have more columns than rows. It is then possible that both matrices have right inverses, in which case both algorithms would yield the correct dynamics, up to computational error. (Problems could arise if the data are correlated in a way so as to make the rows of  $\Omega$  or  $\begin{bmatrix} Z_j \\ \Gamma_j \end{bmatrix}$  linearly dependent.) Note that this also occurs for Example 1.

*Example 3 (Erdős-Renyi random graphs):* To further establish the computational efficiency of Network DMDc, we compared it to the standard DMD algorithm when applied to linear systems whose network structures are Erdős-Renyi random directed graphs. That is, we considered networks produced according to the following process: Fix a probability  $p \in [0, 1]$  and start with a fixed number of vertices  $n$ . Then for every pair of vertices  $(v, v')$ , include a directed edge from  $v$  to  $v'$  with probability  $p$ . These choices of edges are determined independently. All vertices were assumed to be state vertices. Also,  $P_w = \mathbb{R}$  for all  $w \in N$  and the scalars determining the linear transition functions  $T_w$  were chosen randomly from a uniform distribution on  $[-1, 1]$ .

The Network DMDc algorithm was performed as described in the previous example on data generated by simulations of various time lengths of these networks. The resulting matrix models were then compared to those of the DMD (not DMDc since there are no control inputs). As in the previous example, Network DMDc consistently outperformed DMD. For example, for 20 Erdős-Renyi networks having  $n = 50$  vertices and probability  $p = 0.05$  (an example is depicted in Figure 5), the Network DMDc and DMD algorithms yielded average model errors given in Figure 6.

Once again, the Network DMDc algorithm recovered the linear dynamics with data from simulations of relatively short length, namely the length matching the dimension of each network’s largest local subsystem. On the other hand, DMD was unable to recover the dynamics accurately due to singular values too close to 0 (relative to the largest singular value) appearing in the data matrices  $\Omega$  for large simulation lengths. This causes the pseudo-inverse, in our case implemented by the `pinv()` function in the Python Numpy package [34],

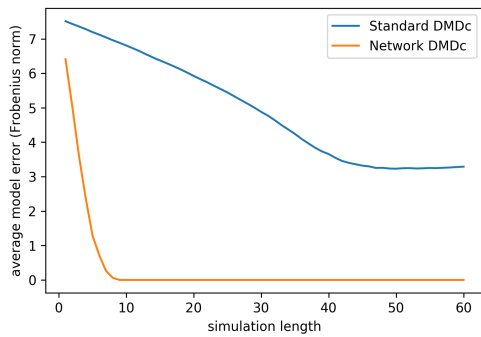


Fig. 6. Average error in the results of the DMD and Network DMDc applied to the 20 Erdős-Renyi random networks with  $n = 50$  and  $p = 0.05$

of the matrix difficult to numerically compute. Note that this is liable to happen for Network DMDc as well, but is significantly mitigated if the local subsystems of the network have low dimension.

The above examples demonstrate the computational benefit of Network DMDc. Its central advantage is its exploitation of the network structure in systems to decompose them into smaller subsystems, which in turn lessens the burden and instability of the linear algebra methods used in DMD and DMDc. We see in particular that these benefits should generally manifest for network structures whose local subsystems have a significantly smaller dimension than that of the system as a whole (e.g., systems whose nodes have few incoming edges relative to the size of the network).

## V. CONCLUSION

In this paper, we have developed a method of applying Koopman theory and dynamic mode decomposition to networked control systems. In particular, we have seen how to decompose the Koopman operator of a networked system into lesser operators, on each of which we can apply the DMDc algorithm. This allows us to obtain numerical approximations for the lesser operators, which can then be composed to produce a linear model for the entire system. We have seen through examples how this process can improve the computation of the resulting models. By focusing on the dynamics associated with each vertex separately and deliberately cutting out computation corresponding to dynamically unconnected components of the system, Network DMDc can accurately recover linear dynamics of networked systems with less data, and thus with a lower computational burden, than standard DMD and DMDc. Additionally, Network DMDc lends itself naturally to parallel computation, which can improve computational efficiency even more. With its ability to also work with nonlinearities, in addition to its possible use in tandem with distributed control algorithms, Network DMDc has great potential to be used in the modeling and control of complex interconnected systems.

## REFERENCES

[1] P. J. Schmid and J. Sesterhenn, “Dynamic mode decomposition of numerical and experimental data,” in *61st Annual Meeting of the APS Division of Fluid Dynamics*. American Physical Society, 2008.

[2] P. J. Schmid, “Dynamic mode decomposition of numerical and experimental data,” *J. Fluid Mech.*, vol. 656, pp. 5–28, 2010.

[3] B. O. Koopman, “Hamiltonian systems and transformation in Hilbert space,” *PNAS*, vol. 17, no. 5, pp. 315–318, 1931.

[4] I. Mezić, “Spectral properties of dynamical systems, model reduction and decompositions,” *Nonlin. Dynam.*, vol. 41, no. 1–3, pp. 309–325, 2005.

[5] C. W. Rowley, I. Mezić, S. Bagheri, P. Schlatter, and D. S. Henningson, “Spectral analysis of nonlinear flows,” *J. Fluid Mech.*, vol. 641, pp. 115–127, 2009.

[6] P. J. Schmid, “Application of the dynamic mode decomposition to experimental data,” *Exp. Fluids*, vol. 50, pp. 1123–1130, 2011.

[7] J. H. Tu, C. W. Rowley, D. M. Luchtenburg, S. L. Brunton, and J. N. Kutz, “On dynamic mode decomposition: theory and applications,” *J. Comput. Dyn.*, vol. 1, no. 2, pp. 391–421, 2014.

[8] I. Mezić, “Analysis of fluid flows via spectral properties of the Koopman operator,” *Annu. Rev. Fluid Mech.*, vol. 45, pp. 357–78, 2013.

[9] Y. Susuki and I. Mezić, “Nonlinear Koopman modes and coherency identification of coupled swing dynamics,” *IEEE Trans. Power Syst.*, vol. 26, no. 4, pp. 1894–1904, 2011.

[10] —, “Nonlinear Koopman modes and a precursor to power system swing instabilities,” *IEEE Trans. Power Syst.*, vol. 27, no. 3, pp. 1182–1191, 2012.

[11] —, “Nonlinear Koopman modes and power system stability assessment without models,” *IEEE Trans. Power Syst.*, vol. 29, no. 2, pp. 899–907, 2014.

[12] Y. Susuki, I. Mezić, F. Raak, and T. Hikiyama, “Applied Koopman operator theory for power systems technology,” *NOLTA, IEICE*, vol. 7, no. 4, pp. 430–459.

[13] J. Grosek and J. N. Kutz, “Dynamic mode decomposition for real-time background/foreground separation in video,” 2014, arXiv:1404.7592.

[14] J. N. Kutz, X. Fu, S. L. Brunton, and J. Grosek, “Dynamic mode decomposition for robust pca with applications to foreground/background subtraction in video streams and multi-resolution analysis,” in *Handbook on robust low-rank and sparse matrix decomposition: Applications in image and video processing*, T. Bouwmans, N. S. Aybat, and E. Hadi Zahzah, Eds. Boca Raton: CRC Press, 2015.

[15] N. B. Erichson and C. Donovan, “Randomized low-rank dynamic mode decomposition for motion detection,” *Computer Vision and Image Understanding*, vol. 146, pp. 40–50, 2016.

[16] J. L. Proctor and P. A. Eckhoff, “Discovering dynamic patterns from infectious disease data using dynamic mode decomposition,” *Int. Health*, vol. 7, no. 2, pp. 139–145, 2015.

[17] E. Berger, M. Sastuba, D. Vogt, B. Jung, and H. B. Amor, “Estimation of perturbations in robotic behavior using dynamic mode decomposition,” vol. 29, no. 5, pp. 331–343, 2015.

[18] B. W. Brunton, L. A. Johnson, J. G. Ojemann, and J. N. Kutz, “Extracting spatial-temporal coherent patterns in large-scale neural recordings using dynamic mode decomposition,” *J. Neurosci. Meth.*, vol. 258, pp. 1–15, 2016.

[19] J. Mann and J. N. Kutz, “Dynamic mode decomposition for financial trading strategies,” *Quant. Finance*, vol. 16, no. 11, pp. 1643–1655, 2016.

[20] M. O. Williams, I. G. Kevrekidis, and C. W. Rowley, “A data-driven approximation of the Koopman operator: extending dynamic mode decomposition,” *J. Nonlinear Sci.*, vol. 25, no. 6, pp. 1307–1346, 2015.

[21] M. O. Williams, C. W. Rowley, and I. G. Kevrekidis, “A kernel-based approach to data-driven koopman spectral analysis,” 2014, arXiv:1411.2260.

[22] J. N. Kutz, X. Fu, and S. L. Brunton, “Multiresolution dynamic mode decomposition,” *SIAM J. Appl. Dyn. Syst.*, vol. 15, no. 2, pp. 713–735, 2016.

[23] M. R. Jovanovic, P. J. Schmid, and J. W. Nichols, “Sparsity-promoting dynamic mode decomposition,” *Phys. Fluids*, vol. 26, 2014, 024103.

[24] S. L. Brunton, J. L. Proctor, and J. N. Kutz, “Compressive sampling and dynamic mode decomposition,” 2013, arXiv:1312.5186.

[25] M. S. Hemati, C. W. Rowley, E. A. Deem, and L. N. Cattafesta, “De-biasing the dynamic mode decomposition for applied Koopman spectral analysis of noisy datasets,” *Theor. Comput. Fluid Dyn.*, 2017.

[26] J. L. Proctor, S. L. Brunton, and J. N. Kutz, “Dynamic mode decomposition with control,” *SIAM J. Appl. Dyn. Syst.*, vol. 15, no. 1, pp. 142–161, 2016.

[27] S. T. M. Dawson, N. K. Schiavone, C. W. Rowley, and D. R. Williams, “A data-driven modeling framework for predicting forces and pressures on a rapidly pitching airfoil,” in *45th AIAA Fluid Dynamics Conference*. American Institute of Aeronautics and Astronautics, 2015.



- [28] J. L. Proctor, S. L. Brunton, and J. N. Kutz, "Generalizing Koopman theory to allow for inputs and control," 2016, arXiv:1602.07647.
- [29] S. L. Brunton, B. W. Brunton, J. L. Proctor, and J. N. Kutz, "Koopman invariant subspaces and finite linear representations of nonlinear dynamical systems for control," *PLoS ONE*, vol. 11, no. 2, 2016, e0150171.
- [30] M. O. Williams, M. S. Hemati, S. T. M. Dawson, I. G. Kevrekidis, and C. W. Rowley, "Extending data-driven Koopman analysis to actuated systems," in *10th IFAC Symposium on Nonlinear Control Systems*. International Federation of Automatic Control, 2016.
- [31] M. Korda and I. Mezić, "Linear predictors for nonlinear dynamical systems: Koopman operator meets model predictive control," 2016, arXiv:1611.03537.
- [32] M. Budišić, R. Mohr, and I. Mezić, "Applied Koopmanism," *Chaos*, vol. 22, no. 4, 2012.
- [33] R. V. Kadison and J. R. Ringrose, *Fundamentals of the theory of operator algebras*, ser. Graduate Studies in Mathematics. Providence, RI: American Mathematical Society, 1997, vol. 15.
- [34] E. Jones, T. Oliphant, P. Peterson *et al.*, "SciPy: Open source scientific tools for Python," 2001–. [Online]. Available: <http://www.scipy.org/>